

Original Article

Effect of Cr Content on the Heat-Treatment of the Alloy for Brake Disc

Gwanhwi Lee¹, Kwonhoo Kim², Jong-Deok Lim² and Hyun-Jong Kim², Je-Pil Wang^{3*}

¹Turbo Power Tech CO. LTD, Dasan-ro, Saha-gu, Busan, Korea

²Department of Metallurgical Engineering, Pukong National University, Busan, Republic of Korea

³Division of Convergence Materials Engineering, Major of Metallurgical Engineering, Department of Marine Convergence Design Engineering(Advanced Materials Engineering), Pukyong National University, Busan, Republic of Korea

^{3*}Corresponding Author : jpwang@pknu.ac.kr

Received: 19 November 2022

Revised: 14 January 2023

Accepted: 16 January 2023

Published: 24 January 2023

Abstract - This study was intended to examine the effect of Cr content on heat treatment by adding Fe-Cr alloy to gray cast iron GC250. Designed alloys with Cr content of 0.1%, 0.2%, and 0.3% were cast using a high-frequency induction furnace to determine the change in physical properties according to the amount of Cr added to the ferroalloy. Normalizing was conducted with a box furnace to remove internal stress and control the structure of the ferroalloy, and nitriding heat treatment was conducted using an atmosphere box furnace to improve the surface hardness of the designed alloy. It was confirmed that the optimal conditions for normalizing are a temperature of 930°C, a time of 8hrs, and an airy atmosphere, and the optimal conditions for nitriding heat treatment are a temperature of 560°C, a time of 5hrs, the atmosphere of N₂ 1.5m³/h, NH₃ 15m³/h, CO₂ 0.3m³/h. As a result of comparing the physical properties of ferroalloy according to the Cr content through the above optimal conditions, the designed alloy with a Cr content of 0.1% achieved a tensile strength of 268 MPa and a surface hardness of HBW 251. Compared to gray cast iron GC250, the tensile strength increased by about 58% and the surface hardness by about 21 %.

Keywords - Gray cast iron, Alloy iron, Casting, Heat- treatment, Tensile strength, Brinell hardness.

1. Introduction

With the rapid development of the automobile industry, the high power output of engines, high fuel efficiency, and weight reduction of vehicles are continuously progressing, leading to a continuous increase in traffic accidents. In response to this trend, the importance of the automobile braking system is rising [1]. The vehicle's braking system is composed of disks and pads. It aims to reduce or stop the moving speed of the automobile by converting the vehicle's kinetic energy into mechanical frictional heat energy with the applied high-pressure load [10]. Under normal driving conditions, the brake repeats braking and driving, and the disk repeats heat generation by friction and heat dissipation due to conduction and convection. Most of the kinetic energy generated during driving is transferred to the brake disc in the form of frictional heat, leading to a sudden increase in the temperature in the contact surface between the disc and the pad. [1].

This temperature increase leads to overheating of the disk, promoting thermal deformation of the disk, which in turn causes cracks, noise, and vibration that deteriorate

braking performance. To solve the deterioration of braking performance, studies on the method of improving abrasion resistance and thermal conductivity, uneven abrasion due to residual stress; the development of disc material to reduce abnormal vibration of brake and improve durability [3][4], the causes of abnormal vibration and solutions; and analysis using computer simulations [12] are in progress. Despite of these efforts to ensure the stability of the brake with the aim of improving the braking performance of the vehicle, shortening the stopping distance and extending the use time, it is difficult to quantitatively and clearly analyze the causes of abnormalities and vibrations of the brake system in actual driving. [6][7][14].

Most of the mass-produced brake disc materials are made of a single material of gray cast iron, with excellent heat dissipation performance and durability. Commercial brake discs are manufactured by adding various alloying elements to prevent thermal deformation, improve braking performance, and reduce noise and vibration. Studies on improving disc performance by adding Ni, Cr, Mo, and rare earth elements are also in progress.



In this study, gray cast iron used as a material for automobile brake discs and Cr, a representative alloying element that affects the properties of cast iron (abrasion resistance and operability), was melted and cast together, and changes in the physical properties of the material according to the Cr content were observed. In addition, changes in material properties alloying elements according to microstructure control were observed by treating the material with heat.

2. Materials

The microstructure picture, chemical composition, and physical properties of gray cast iron GC250 used in this study are presented in (Figure 1). For analysis, the raw material in the shape of a rod was cut using a high-speed cutter and then processed for tensile test, Brinell hardness test, and SEM (Scanning Electron Microscope), XRF (X-Ray Fluorescence), C /S (Carbon/Sulfur) analysis. As a result of the analysis, it was confirmed that 92.99% of Fe, 3.53% of C, and 2.69% of Si were present as main elements and trace amounts of Mn, S, and P were present in the raw material, and that the carbon in the pearlite matrix was a microstructure in the form of flake graphite. In addition, as a result of testing the physical properties of the raw material, it was confirmed that the tensile strength was 169 MPa, and Brinell hardness was HBW 207.

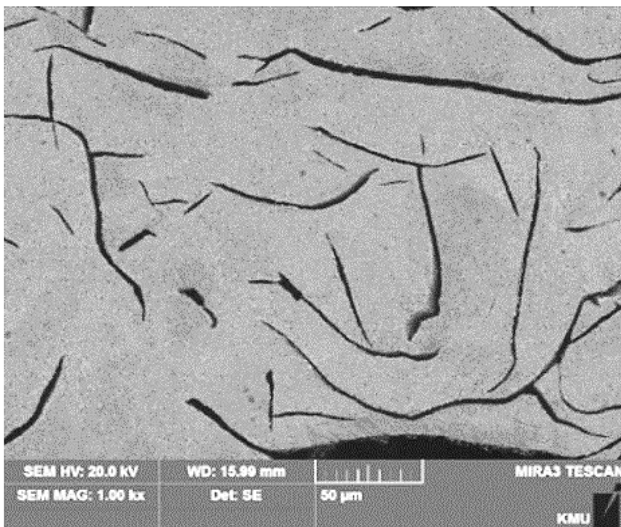


Fig. 1 Microstructure picture of gray cast iron GC250

Table 1. Chemical composition and properties of gray cast iron GC250

XRF		Tensile Strength
Element	wt.%	
Fe	92.99	169 MPa
C	3.53	
Si	2.69	
Mn	0.64	Brinell Hardness
S	0.08	
P	0.07	HBW 207

3. Experiment Method

By referring to the composition of ferroalloy Fe-Cr (Fig. 2), the weight ratio of gray cast iron GC250 and ferroalloy Fe-Cr was matched and blended. Then it was melted in an Ar atmosphere using a high-frequency induction furnace. A Y-block with a thickness of 70mm and a length of 230mm was cast by tapping the molten metal after mixing the ingredients. XRF and C/S analysis were conducted to determine the chemical composition of the cast material, and SEM was used to observe the microstructure. In addition, a tensile test and a Brinell hardness test were conducted to determine the physical properties of the cast alloy. In addition, normalizing was conducted at 930°C for 8 hrs in an air atmosphere to control the microstructure of the cast material and remove internal stress. Nitriding heat treatment was conducted at a temperature of 560°C for 5 hrs in the atmosphere of N2 1, 5m3/h, NH3 15m3/h, CO2 0.3m3/h.

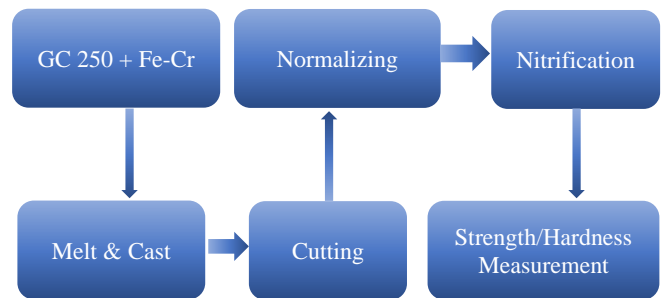


Fig. 2 Full experimental flow chart

Table 2. Composition of ferroalloy Fe-Cr

Fe-Cr Composition	
Element	%
Cr	60 min.
Si	4 max
C	0.1 max
S	0.03 max
P	0.04 ax

4. Results and Discussion

4.1. Alloy Designs

By using a high-frequency induction furnace, gray cast iron GC250 and alloy iron Fe-Cr were calculated by the weight ratio presented in (Figure 2). and mixed, then melted and cast at a temperature of 1600°C for 30 min in an Ar atmosphere. To observe the change in physical properties of the designed alloy according to the content, Y-blocks with Cr content of 0.1%, 0.2%, and 0.3% were cast, respectively. XRF and C/S analysis were conducted to determine the chemical composition of the cast material, and SEM was taken to observe the microstructure of the cast alloy. In addition, the Brinell hardness and tensile tests observed the change in the physical properties according to the Cr content of the designed alloy.

Table 3. Chemical composition of the cast design alloy

Unit: wt.%

Element Sample	C	Si	Mn	P	S	Cr	Mo	Cu	Fe
Cr 0	3.53	2.68	0.64	0.07	0.08	-	-	-	Bal
Cr 0.1	3.28	2.7	0.413	0.052	0.053	0.096	0.013	0.027	Bal
Cr 0.2	3.3	2.73	0.407	0.053	0.053	0.184	0.023	0.03	Bal
Cr 0.3	3.35	2.75	0.41	0.057	0.051	0.289	0.026	0.033	Bal

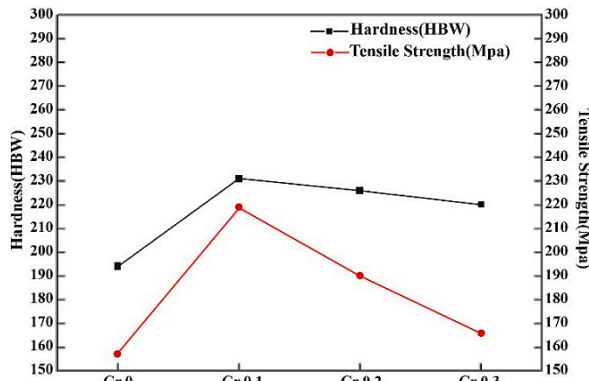


Fig. 3 Physical properties of the designed alloy

Table 4. Physical properties of the designed alloy

Sample	Hardness	Strength	
		Tensile Strength	Yield Strength
Cr 0	194 HBW	157 MPa	125 MPa
Cr 0.1	231 HBW	219 MPa	182 MPa
Cr 0.2	226 HBW	190 MPa	128 MPa
Cr 0.3	220 HBW	166 MPa	128 MPa

The chemical composition analysis results of the cast alloy material s for each Cr content were presented in Table 1. As a result of XRF analysis, the Cr content was measured to be 0.096 wt.%, 0.184 wt.%, and 0.289 wt.%, respectively. It was confirmed that the target Cr-added alloy was manufactured through component analysis.

The results of the physical property analysis of the designed alloy by Cr content are presented in Fig 3. As a result of the analysis, it was confirmed that physical properties such as surface hardness, tensile strength, and yield strength increased with Cr content added compared to the raw material. However, as the amount of Cr added increased, the physical properties tended to decrease, indicating that adding an appropriate amount of Cr in the gray cast iron alloy helps improve the properties of the designed alloy.

The microstructure of the Y-block after casting was observed through an optical microscope (OM), and the microstructure pictures were presented in Fig 4. As a result of the analysis, pearlite matrix and flake graphite structures were observed in the raw material, whereas ferrite matrix and flake graphite structures were observed in the structure of the designed alloy. It is considered that this change in the matrix structure was due to the addition of alloying elements and the effect of casting.

4.2. Heat Treatment

To control the microstructure of the cast-designed alloy and remove the internal stress, normalizing was conducted using a box furnace at a temperate of 930°C for 2hrs/4hrs/8hrs in an air atmosphere using a box furnace. The microstructure pictures observed using an optical microscope (OM) after normalizing are presented in Fig 5. As a result of observing the alloy's microstructure, it was confirmed that the microstructure did not change in the structure normalized for 2hrs and 4hrs, and the matrix structure was pearlitized after normalizing for 8hrs. In addition, it was confirmed that the

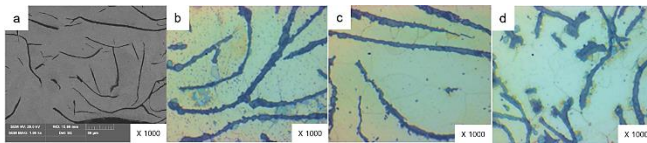


Fig. 4 a)Raw material, b) Cr 0.1%, c) Cr 0.2%, d) Cr 0.3%

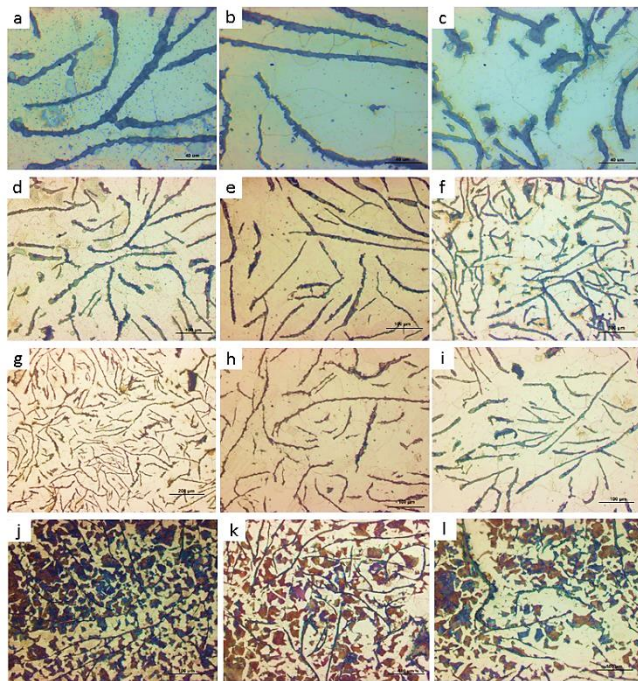


Fig 5. a) Cr 0.1%, b) Cr 0.2%, c) Cr 0.3% - before heat treatment
 d) Cr 0.1%, e) Cr 0.2%, f) Cr 0.3% - after heat treatment_2h
 g) Cr 0.1%, h) Cr 0.2%, i) Cr 0.3% - after heat treatment_4h
 j) Cr 0.1%, k) Cr 0.2%, l) Cr 0.3% - after heat treatment_8h

pearlite structure fraction was formed more densely as the Cr content decreased.

4.3. Nitriding Heat Treatment

The alloy used for the nitriding heat treatment was an alloy whose matrix structure had been changed after normalizing for 8 hrs. To improve the physical properties of the normalized material, nitriding heat treatment was conducted using an atmosphere box furnace. Nitriding heat treatment was conducted at 560°C, a temperature range in which the phase change of the cast iron structure does not occur, in an atmosphere of N₂ 1.5m³/h, NH₃ 15m³/h, CO₂ 0.3m³/h referring to the nitriding atmosphere, which is a normal practice. In addition, the material was retained for 5 hrs to induce sufficient nitride layer formed on the material surface.

To observe the material's physical properties change after nitriding heat treatment, the Brinell hardness test and tensile test were conducted, and the results are presented in Fig 7. As a result of the test, it was confirmed that the surface hardness of the alloy increased by forming a surface nitride layer after nitriding heat treatment. In the case of strength, the result was similar to the value obtained by normalizing for 8hrs, and the nitriding heat treatment did not affect the strength.

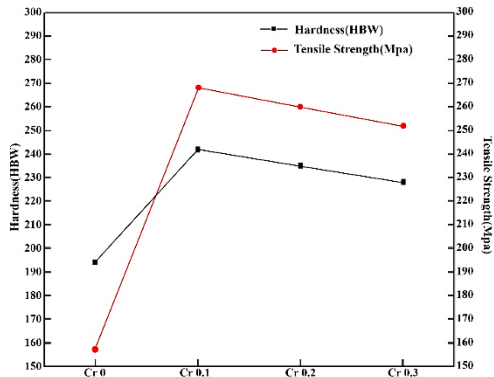


Fig. 6 Physical properties of the designed alloy after normalizing for 8 hrs

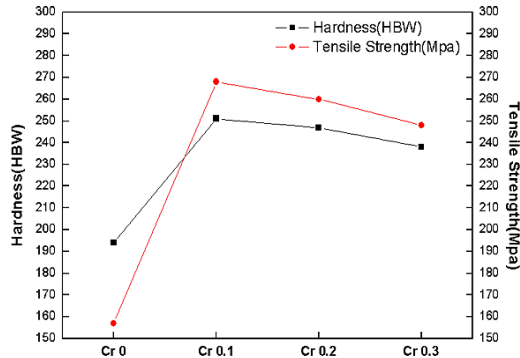


Fig. 7 Physical properties of the designed alloy after nitriding heat treatment

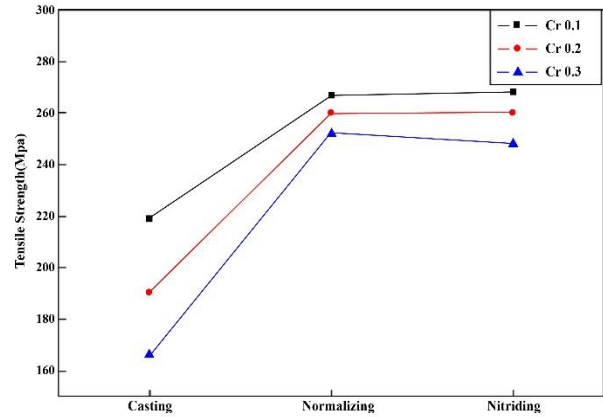


Fig. 8 a Changes in tensile strength of the designed alloy

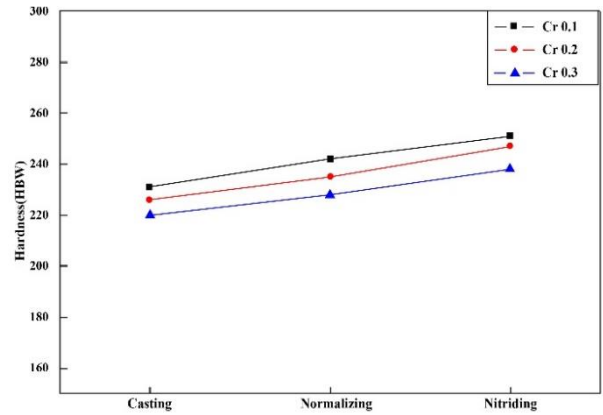


Fig. 8 b Changes in Hardness of the designed alloy

Fig. 8a & b Changes in physical properties of the designed alloy according to the amount of Cr added

The test results of the change in the designed alloy properties according to the amount of Cr added are presented in Fig 8. The change in the physical properties of the cast alloy after normalizing and after nitriding heat treatment were compared. The overall hardness and strength were high under the condition of 0.1%, in which the Cr content was the least added. Also, in the case of surface hardness and tensile strength, normalizing for 8 hrs and nitriding heat treatment were conducted. The results confirmed that the surface hardness was improved by 21% compared to the existing alloy, and the tensile strength was improved by 58% compared to the existing alloy. In addition, the nitriding heat treatment showed a positive effect on the surface hardness of the material, and it was confirmed that there was no significant effect on the improvement of the strength. In some cases, there was a decrease to an extent.

Table 5. Physical properties of the designed alloy after normalizing

Sample	Hardness	Strength	
		Tensile Strength	Yield Strength
Cr 0	194 HBW	157 MPa	125 MPa
Cr 0.1	242 HBW	267 MPa	211 MPa
Cr 0.2	235 HBW	260 MPa	202 MPa
Cr 0.3	228 HBW	252 MPa	192 MPa

Table 6. Physical properties of the designed alloy after nitriding heat treatment

Sample	Hardness	Strength	
		Tensile Strength	Yield Strength
Cr 0	194 HBW	157 MPa	125 MPa
Cr 0.1	251 HBW	268 MPa	222 MPa
Cr 0.2	247 HBW	260 MPa	194 MPa
Cr 0.3	238 HBW	248 MPa	185 MPa

5. Conclusion

In this study, a designed alloy was manufactured by melting gray cast iron GC250 and ferroalloy Fe-Cr to improve the properties of alloy materials for automobile brake discs. To improve the physical properties of the designed alloy, the optimal process conditions for the amount of Cr added and normalizing time was determined, and the

effect of the nitride layer formed on the material surface was examined through nitriding heat treatment.

As a result of the experiment, it was confirmed that the optimal process conditions to improve the material properties were at a temperature of 930°C for 8 hrs with the content of 0.1%, nitriding heat treatment after normalizing at a temperature of 560°C for 5 hrs in an air atmospheric, and in an atmosphere of N₂ 1.5m³/h, NH₃ 15m³/ h, CO₂, and 0.3m³/h, where the tensile strength of the designed alloy was 268 MPa and the surface hardness was HBW 251.

Acknowledgments

This work was supported by the Technology Development Program (CD202111550001), funded by the Ministry of SMEs and Startups (MSS, Korea).

References

- [1] Ma, Jeong-Beom, and Lee, Bong-Gu, "Thermal Behavior of Ventilated Disc Brakes Considering Contact Between Disc and Pad," *Journal of the Korean Society of Manufacturing Technology Engineers*, vol. 23, no. 3, pp. 259-265, 2014. *Crossref*, <https://doi.org/10.7735/ksmte.2014.23.3.259>
- [2] N.Saravana Kumar et al., "Experimental Investigation on Mechanical Behavior of E-Glass and S-Glass Fiber Reinforced with Polyester Resin," *SSRG International Journal of Mechanical Engineering*, vol. 5, no. 5, pp. 19-26, 2018. *Crossref*, <https://doi.org/10.14445/23488360/IJME-V5I5P104>
- [3] Masahiro Kubota et al., "Development of a Light Brake Disk Rotor: a Design Approach for Achieving an Optimal Thermal, Vibration and Weight Balance," *Japanese Society of Automotive Engineers Review*, vol. 21, no. 3, pp. 349-355, 2000. *Crossref*, [http://dx.doi.org/10.1016/S0389-4304\(00\)00050-3](http://dx.doi.org/10.1016/S0389-4304(00)00050-3)
- [4] Taein Yeo, "A study on Wear Life Prediction of Disk Brake pads," *KSAE*, vol. 10, no. 4, pp. 199-200, 2002
- [5] V.Naga Malleswari, and R. Padmini, "Evaluation of Mechanical Properties of Aluminium Metal Matrix Reinforced with Silicon," *SSRG International Journal of Mechanical Engineering*, vol. 5, no. 1, pp. 14-18, 2018. *Crossref*, <https://doi.org/10.14445/23488360/IJME-V5I1P103>
- [6] Armin Yazdandshenas, and Chung-Hyun Goh, "Rockwell Hardness Testing on an Aluminum Specimen Using Finite Element Analysis," *SSRG International Journal of Mechanical Engineering*, vol. 7, no. 4, pp. 1-10, 2020. *Crossref*, <https://doi.org/10.14445/23488360/IJME-V7I4P101>
- [7] Anthony J. Hayter, "A Proof of the Conjecture that the Tukey-Kramer Multiple Comparisons Procedure is Conservative," *Annals of Statistics*, vol. 12, no. 1, pp. 61-75, 1984. *Crossref*, <https://doi.org/10.1214/aos/1176346392>
- [8] K. John Joshua, P. Sherjin, and J. Perinba Selvin Raj, "Analysis of Ball Milled Aluminium Alloy 7068 Metal Powders," *SSRG International Journal of Mechanical Engineering*, vol. 4, no. 8, pp. 6-10, 2017. *Crossref*, <https://doi.org/10.14445/23488360/IJME-V4I8P102>
- [9] S. Chandrasekaran, M. V. Khemchandani, and J. P. Sharma, "Effect of Abrasive Contaminants on Scuffing," *Tribology International*, vol. 18, no. 4, pp. 219-222, 1985. *Crossref*, [https://doi.org/10.1016/0301-679X\(85\)90065-9](https://doi.org/10.1016/0301-679X(85)90065-9)
- [10] Rajneesh Kumar et al., "Evaluation of Mechanical and Microstructural Properties of Cast Iron with Effect of Pre Heat and Post Weld Heat Treatment," *SSRG International Journal of Mechanical Engineering*, vol. 4, no. 5, pp. 1-6, 2017. *Crossref*, <https://doi.org/10.14445/23488360/IJME-V4I5P101>
- [11] Won-jun Cho, A Study on Wear Resistance of Automobile Brake Disc Using Case Hardening, Dong-A University Graduate School of Education, 2015
- [12] Robert E. Bechhofer, and Charles W. Dunnett, *Percentage Points of Multi-variate Student Distributions, Selected Tables in Thematical Studies*, American Mathematical Society, Providence, R. I., vol.11, pp. 57-87, 1988.
- [13] Ko, Y., and Hosoi, K., "Measurements of Power Losses in Automobile Drive Train," *SAE Paper*, 1984. *Crossref*, <https://doi.org/10.4271/840054>
- [14] A.V.L.N.S.H.Hariharan, and Shaik Lakshman, "Analysis of Heavy Metals in the Vicinity of FACOR, Vizianagaram Dt.(AP)," *SSRG International Journal of Applied Chemistry*, vol. 7, no. 1, pp. 56-59, 2020. *Crossref*, <https://doi.org/10.14445/23939133/IJAC-V7I1P111>